The Role of Carbonate-Host Rocks on the Genesis of Pb-Zn Deposits, Northern Thrust Zone, Kurdistan Region, Iraq

Waleed S. Shingaly[1]*, Ali I. Al-Juboury[2], Elias M. Elias[2]

1- Dept. of Geology, College of Science, Salahaddin University, Erbil, Iraq.
2- Dept. of Earth Sciences, College of Science, Mosul University, Mosul, Iraq.

* Corresponding Author: waleed_0076@yahoo.com

Received: 08 November 2014 / Accepted: 05February2015 / Published online: 08February 2015

Abstract

Pb-Zn deposits in the Kurdistan Region, northern Iraq, have occurred mainly as a stratabound and open-space filling ore bodies. They are hosted by dolostone and dolomitic-limestone of platform carbonates. The ore deposits at the studied Dure and Lefan areas are respectively hosted by Kurra Chine (upper Triassic) and Bekhme (upper Cretaceous) formations. Pyrite, sphalerite and galena are the major sulfides minerals, but the mineral paragenesis and relative proportions of these sulfides vary from deposit to other. They have commonly been deposited through dissolution/replacement process and/or through void infilling. Homogenization temperatures of primary and secondary fluid inclusions in Dure and Lefan deposits range from 45 ^{o}C to 183 ^{o}C and from 68^{o}C to 284 ^{o}C, respectively. The salinity is ranging from 13.93 wt% NaCl equiv. to >23 wt% NaCl equiv. in Dure deposit, and from 3.06 wt% NaCl equiv. to 14.57 wt% NaCl equiv. in Lefan deposit. The average δ^{34}S‰ values for sulfide minerals (pyrite, sphalerite and galena) of the Dure and Lefan deposits are -0.8 ‰ and 1.8 ‰, respectively. Sulfur isotope analysis implies that the sulfur in sulfide deposits is originated from a mixture of different sources. The δ^{13}C and δ^{18}O values of carbonate host rocks fall in the range of marine carbonates. Petrographic evidence and stable isotope data with fluid inclusions suggest that Pb-Zn mineralization was caused by deeply circulating high temperature mineralizing fluids (brines) within the source basin or by tectonic processes, which possibly leached metals from either the diagenesis of host rocks and/or the dewatering of deeper buried siliciclastic beds. The studied carbonate-hosted Pb-Zn deposits share many similarities with the Mississippi Valley Type (MVT) deposit.

Keywords: Carbonate rocks, Pb-Zn deposit, Fluid inclusions, Stable isotopes, Iraq.

1–Introduction

Since the fifties of the last century, many studies have been carried out in the Kurdistan Region, northern Iraq for studying the mineral deposits (Jassim and Goff, 2006). Pb-Zn deposits in the Northern Thrust Zone in the Kurdistan Region of Iraq occur mainly in two districts (Vanecek, 1972); (i) the western district northeast of Zakho and (ii) the eastern district to the north of Amadiyah (Fig. 1). The western district includes several occurrences of sulfide with minor barite mineralization. The most important of these deposits are the Berzanik, Alanish, Patruma, Marssis, Lefan, Banik and Shiranish Islam of which the present study focused on the Lefan area. In the eastern district, the largest known sulfide deposits of the Northern Thrust Zone are in the Duri Serguza, which was named by Dure section in the present study according to the current name of this village. However, two sections of carbonate-hosted Pb-Zn sulphide have been chosen in this study; the Dure (Duri Serguza) in the east and the Lefan in the west (Fig. 1). Mineralization of the Northern Thrust Zone is characterized by simple mineralogy (i.e. pyrite, sphalerite and galena) distributed essentially within Mesozoic carbonate sedimentary rocks. Although this sedimentary succession is associated with tectonic zones especially a regional thrust fault, it is not association with any intrusive or extrusive igneous rocks. Carbonate host rocks in this Zone consist of dolostone to dolomitic limestone with brecciated zones (Jassim and Goff, 2006). There is a little information available to explain the role of carbonate host rocks on the genesis of Pb-Zn deposits in the Northern Thrust Zone in the Kurdistan Region, Iraq. Therefore, this study aims to understand the role of carbonate-host rocks on the genesis of Pb-Zn deposits based on petrographic and geochemical characteristics such as fluid inclusions, sulfur, oxygen and carbon isotopes.

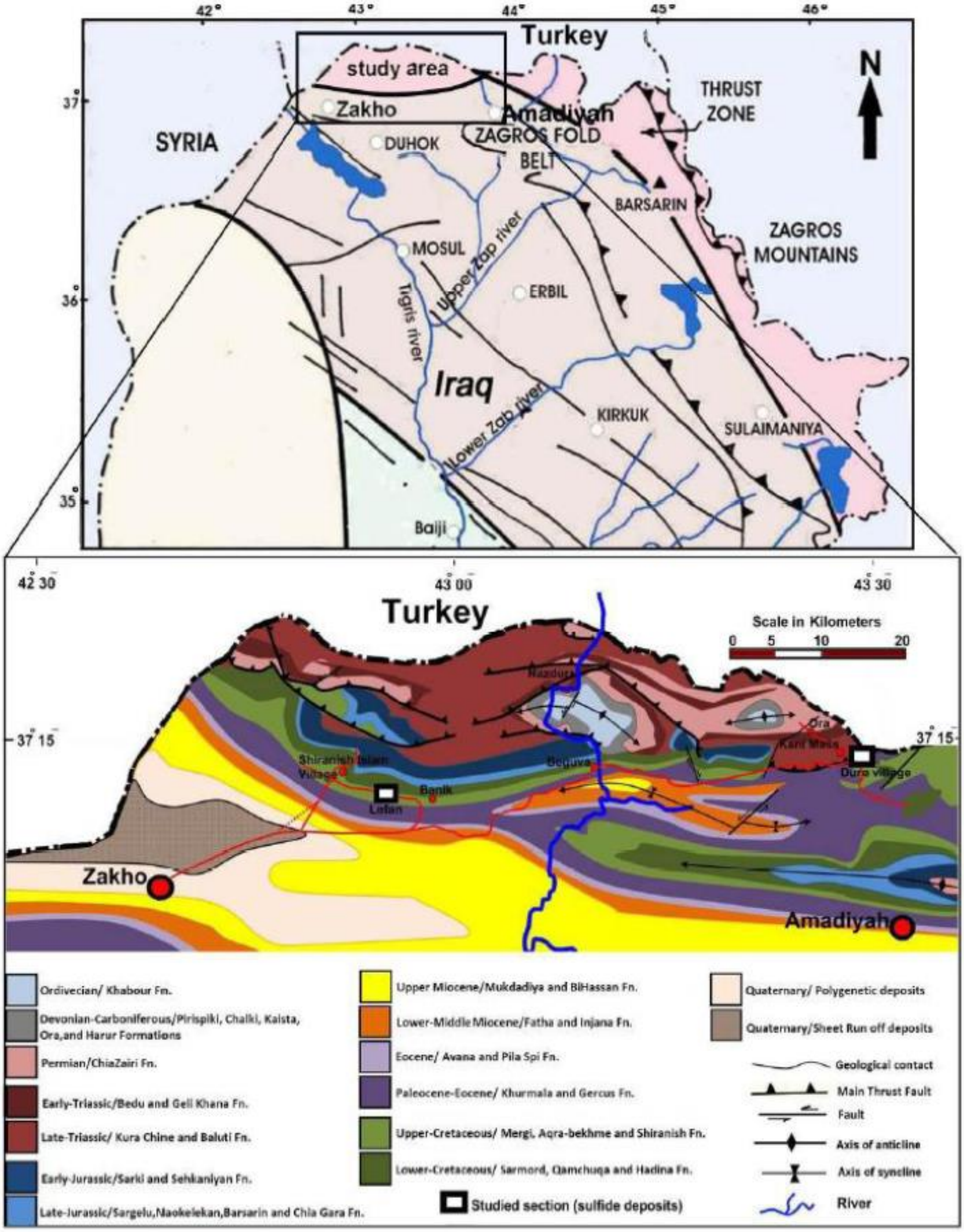

Figure 1)Geological map of the Northern Thrust Zone (modified from Sissakian, 2000) shows the location of the studied sections.

2–Geological Setting

The geologic evolution of the Kurdistan Region is strongly affected by the structural position of Iraq within the main geostructural units of the Middle East; Arabian part of the African platform and the Asian branches of the Alpine geosyncline; as well as by the structure of the country itself. The present-day structural pattern and the individual tectonic units of Iraq are the results of a long-lasting and very complex evolution starting with the Precambrian orogenies and ending with the latest phases of the Alpine Orogeny (Buday and Jassim, 1987). Geology and mineralization of the study area are strongly influenced by the location of the two Phanerozoic geotectonic units (Arabian part of the African platform and the Asian branches of the Alpine geosyncline) and the opening and closing of the Paleo-Tethys and Neo-Tethys. From Late Permian to mid-Cretaceous time, the northeastern Arabian Plate was a gradually subsiding passive margin bordering the Neo-Tethys Ocean (Alsharhan and Nairn, 1997; Sharland *et al*., 2001). The Northern Thrust Zone represents a ridge that developed at the plate margin whereas the Zagros Suture formed within the Neo-Tethyan oceanic domain. Moreover, the Arabian Plate basin was asymmetric with a gentle slope to the east and a maximum depth reached in a foredeep setting in front of the Zagros collision zone. No obvious foredeep is developed along the northern plate boundary, reflecting the escape tectonics of the Anatolian Plate (Turkey). However, the study area is a part of the Northern Taurus Fold – Thrust Belt, which is developed from colliding of Arabian and Eurasian Plates and sedimentary fills of the Neo-Tethys basin. The Northern Thrust Zone, which includes the studied sections, is wide in the west with asymmetrical domal culminations toward the south and occasionally the southern limbs are overturned (Fig. 1). The northern limbs of the structures have lower dips and are cut by reverse faults. Thrusting fault formation is thought to be the last stage of the tectonic movements, but this suggestion was later criticized by Akef (1972) who proved the presence of many crush zones cutting the thrust and probably they are younger than the major thrust. Following this stage the whole area was uplifted to form the present high mountains in the area. In the study area, mineralization zone extends parallel to the bedding plane and exposed on the southern limb of anticlines, striking E–W. Additionally, numerous normal and reverse faults and secondary folds within the existing formations characterize the studied areas. All these structural features led to distortion in the stratigraphic succession of the area.

3–Stratigraphy and Depositional Environments

The area which includes the Dure section is built of Middle and Upper Triassic limestones and dolostones thrusted over Tertiary mudstones and siltstones. The Triassic rocks consist of hard, brecciated cliff-forming dolomitic limestones of the Geli Khana Formation (middle Triassic) and hard, dark gray dolomitic limestones of the Kurra Chine Formation (upper Triassic). The Tertiary succession is weathered and consists of interbedded red and olive green sandstones and mudstones of the Gercus Formation (Miocene) (Fig. 2). Triassic rocks form the high mountains and cliffs in the area; whereas the Tertiary rocks form the lower plains and valleys. The sulfide ore body is hosted within the upper Triassic rocks of the Kurra Chine Formation near the tectonic contact between the Tertiary and Triassic rock units. Facies analysis shows that the sediments of the Kurra Chine Formation in the Dure section were deposited in a peritidal environment under evaporitic conditions, similar to the carbonate-evaporite sequence described by Wilson (1975) with modifications of Flügel (2004). This environment included tidal flats, restricted lagoons, sand shoal and shallow shelf. Aqrawi *et al*. (2010) suggested that the Kurra Chine Formation was probably deposited on an epeiric platform, dominated by subtidal to supratidal cycles with local development of sabkhas. Furthermore, Al-Ameri *et al*. (2009) revealed that the Kurra Chine Formation was probably deposited in a restricted lagoonal environment.

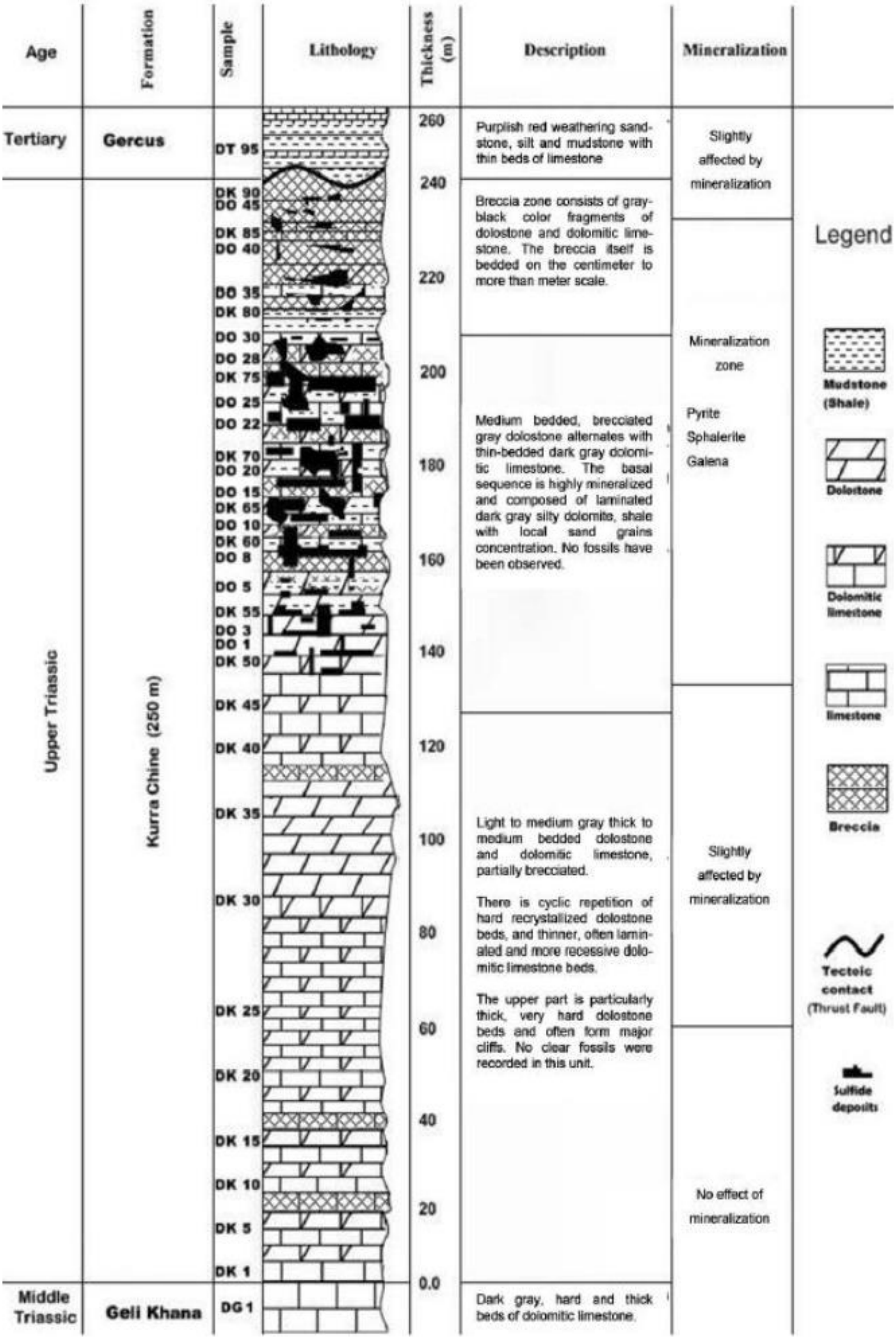

Figure 2) Stratigraphic column of the Kurra Chine Formation showing position of sulfide mineralization in the Dure section. DK: the Dure KurraChine Fm. (Host rock sample), DO: the Dure Ore-sulfides (Ore sample).

In the Lefan section, the formations which are cropping out in the area are Qamchuqa, Mergi, Bekhme and Shiranish. According to Bellen *et al*., (1959) and Buday (1980); the Qamchuqa Formation (middle Cretaceous) consists of massive, argillaceous dolomitic limestone; the

Mergi Formation (middle Cretaceous) is composed of massive, thick-bedded limestone; the Bekhme limestone Formation (upper Campanian) consists of bituminous massive dolomitic limestone. The Shiranish Formation (upper Campanian-Maastrichtian) is composed of blue marl in its upper part and of thin bedded marly limestone in the lower part. The sulfide ore body is hosted mainly within massive limestones of the Bekhme Formation (Fig. 3).

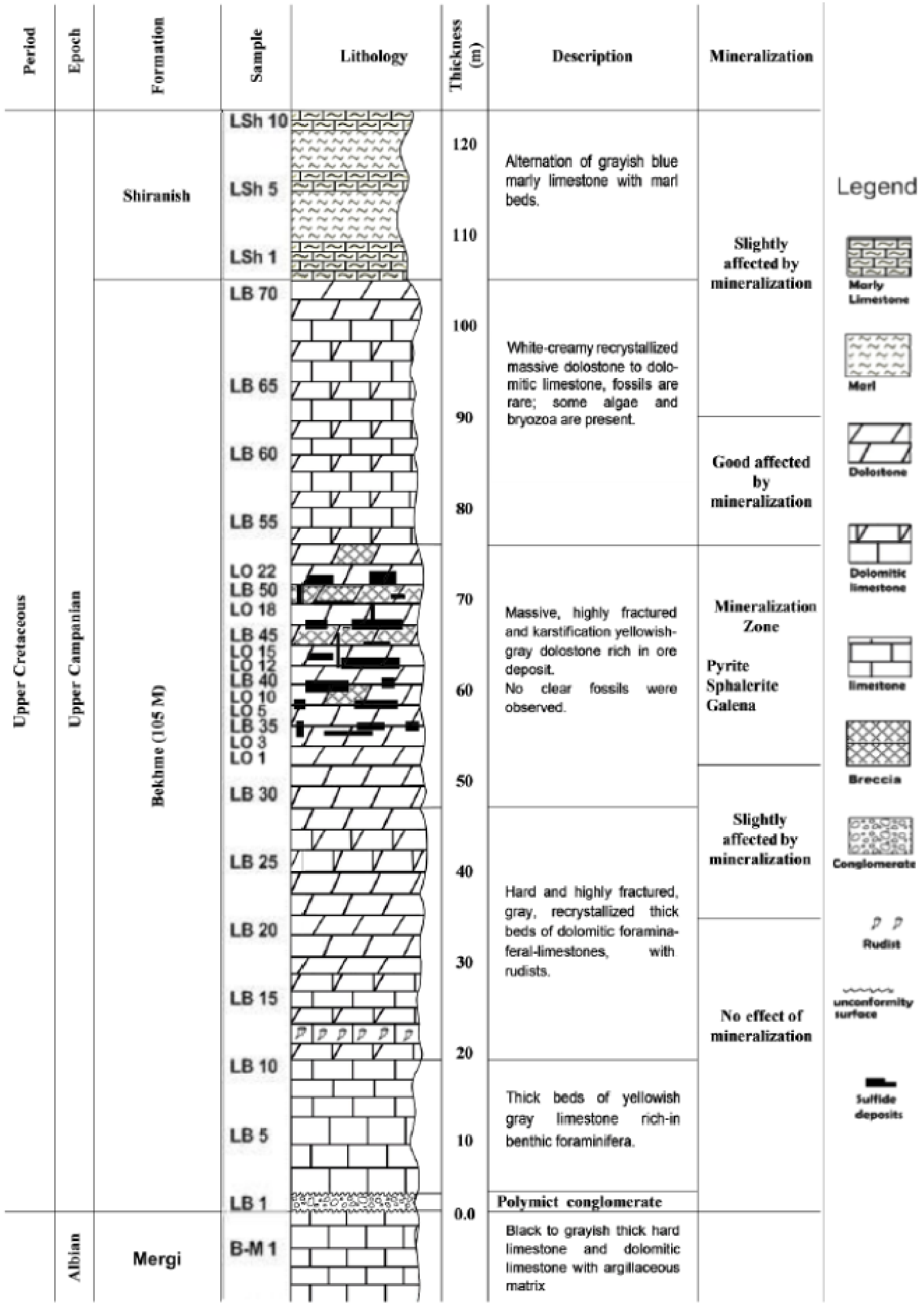

Figure 3) Stratigraphic column of the Bekhme Formation and lower part of the Shiranish Formation showing position of sulfide mineralization in the Lefan section. LB: the Lefan Bekhme Fm. (Host rock sample), LO: Lefan Ore-sulfide (Ore sample).

Taking the terms of facies analysis in to consideration, three main depositional environments were identified in the Bekhme Formation, they are: Lagoon/back reef, reef and forereef spreads distantly from the reef body into deep marine basin sediments (Marl lithofacies) in the contact with the Shiranish Formation, in addition to the carbonate-conglomerate facies at the base of the formation (Fig. 3). Bellen *et al*. (1959) revealed that the Bekhme Formation comprises reef limestones, forereef and shoal limestones, Jassim and Goff (2006) stated that the Bekhme Formation was deposited mostly in a reef-forereef environment.

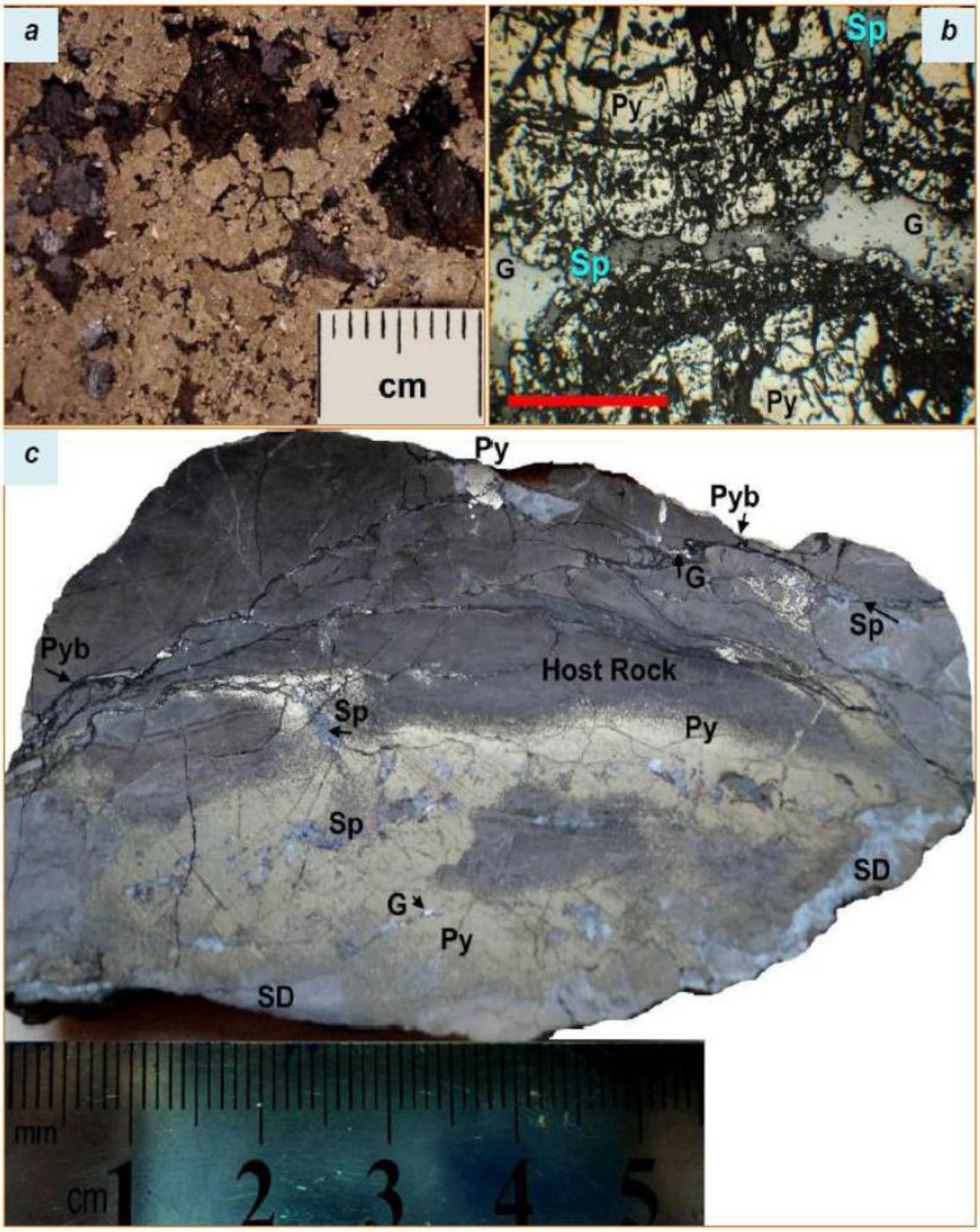

Figure 4) Massive ore body occurrence in the Dure section. a) Sulfide assemblage seen in hand specimens collected from massive ore body. Large, coarse aggregates of sphalerite (brown) are surrounded primarily by pyrite (brass-yellow). Galena (silver-gray) is also present. Photomacrograph, hand sample, (DO 26). b) Veins in massive pyrite (Py) are filled by sphalerite (Sp) and galena (G). Photomicrograph, reflected light, scale bar is 1mm. (DO 10). c) Alternation of sub-millimeter to centimeter bands of pyrite (Py) and thin sphalerite (Sp) with disseminated galena (G) shows a banded structure hosted by gray dolostone. Thin vein filled by pyrobitumen (Pyb) and saddle dolomite (SD) are also present. Photomacrograph, hand sample (DO 11).

4–Pb-Zn Deposits

The ore body in the Dure section occurs as a stratabound demarcates the unconformity between the upper Triassic dolostones of the

Kurra Chine Formation and overlying Tertiary rock units. The Dure ore deposits occur as: massive, banded and vein-type style of mineralization. The ore body consists of massive pyrite with small veins and patches of sphalerite and galena (Figs. 4a,b), which are highly deformed, brecciated, and recrystallized. The banded structure is characterized by an alternation of sub-millimeter (laminations) to centimeter bands (Fig. 4c). The main-stage of mineralization involved the progressive replacement of pre-existing iron sulfides and the dolostone breccias, initially by replacement of the breccia matrix and ultimately by replacement of clasts. The sulfides are intermixed with dolomite (Fig. 4c), whereas calcite is more frequent in the oxidized zone. Petrographic observations of polished sections and XRD indicate that ore minerals in the Dure section (Fig. 5) consist of pyrite, sphalerite, galena, goethite, smithsonite, cerussite and anglesite.

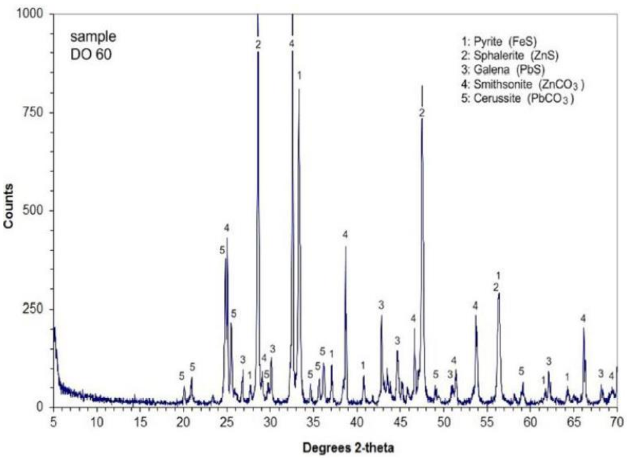

Figure 5) XRD pattern of bulk-ore sample from the Dure section.

Pb-Zn deposit in the Lefan is strata-bound sulfides hosted in the Upper Cretaceous dolomitic limestone of the Bekhme Formation and occurs mainly as open-space fillings or lodes within fractures (Figs. 6a,b). They can be described as tabular fracture fillings and replacement-type ores. These vein-type bodies vary in width from few centimeters up to 2 meters. They are discontinuous along strike and extend into the country rock for several tens of meters. Coarse crystalline sphalerite and galena occur as open space and fracture-fill mineralization within the main ore-stage assemblages where they occur with euhedral dolomite and calcite (Figs. 6c,d). Barite was reported by Awadh (2006) to occur in association with ore and sometimes as an independent mineral in veins, but in the present study it has been observed only in small veins (Fig. 6b). Ore minerals in the Lefan section consist, in decreasing order of abundance, of sphalerite, galena, and minor pyrite, goethite, smithsonite, and cerussite (Fig. 7).

5–Methodology

A total of 165 samples of the carbonate-host rocks and 67 samples from sulfide ore bodies were collected from the studied sections (Figs 2 and 3). Carbonate samples were stained with Alizarin red S following the technique of Dickson (1965) to distinguish between calcite and dolomite. All-thin sections were examined under an optical microscope. Fourteen polished sections of ores were also prepared for mineral identification and textural interpretation. The mineralogy and textures of the samples were determined using reflected and transmitted light microscopy. Representative samples were analyzed for their mineralogical composition by X-ray diffraction (XRD). X-ray diffractionanalyses were performed using a Philips X-ray diffractometer (PW3710) with CuKa radiation and a scanning speed of 4º to 60º 2θ at the department of Earth Sciences, Wollongong University, Australia and the Royal Holloway of London University, UK. Fluid inclusion data have been obtained from 8 double polished-thin sections of ore-stage carbonates (dolomite and calcite) and sphalerite. The microthermometric measurements were performed on a NIKON Labophot-pol microscope mounted with LINKAM THMS-600 and TMS-92 freezing-heating stage and long distance LW40x objective, in the Mineral Processing Research Center (IMPRC), Iran and one sample was also carried out at the Geological Engineering Department of Cumhuriyet University in Sivas,Turkey.

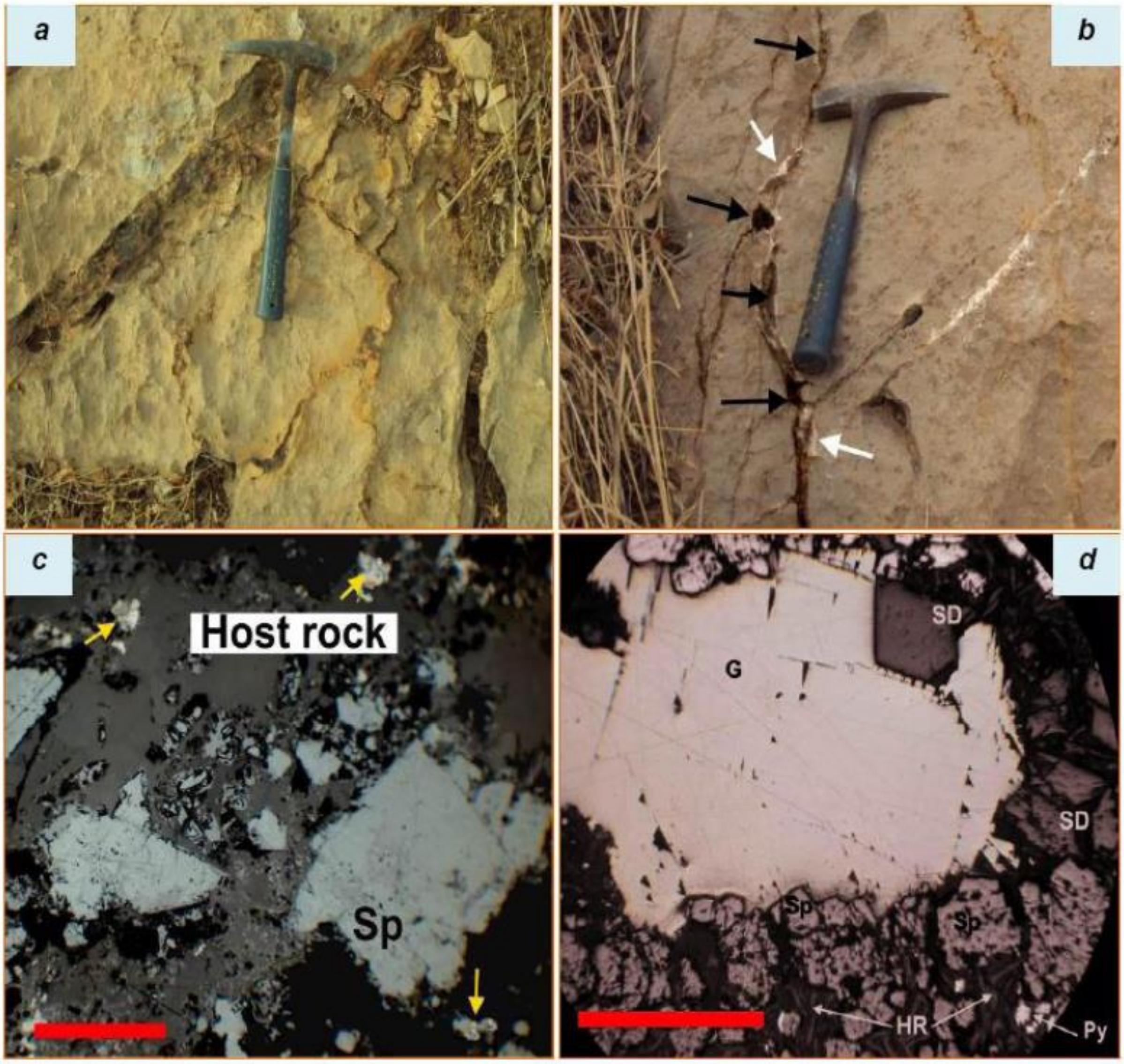

Figure 6) Shape of sulfide–ore body at the Lefan area. a) Open-space fillings and lodes of sulfides within fractures. Note the alteration of sulfides into goethite. Field photograph, geological hummer is a scale. b) Vein-type sulfide bodies, the thin vein of barite (white arrows) cuts the sulfides (black arrows). Field photograph, geological hummer is a scale. c) Early sphalerite (Sp) and fine-grained pyrite (yellow arrows) filled the intergranular dolomite porosity (host rock). Sphalerite shows anhedral to subhedral crystals. Photomicrograph, reflected light, scale bar is 1 mm. (LO 11). d) Open space within main ore-stage assemblage is filled with coarse-grained galena (G) and sphalerite (Sp). Note how galena is surrounded by sphalerite and how host rock (HR) replaced by sphalerite. Saddle dolomite (SD) and pyrite (Py) are also present. Photomicrograph, reflected light, scale bar is 1mm. (DO 18).

Mineral separates for sulfur isotope analysis were acquired by handpicking, checked for purity under a binocular microscope, and hand-ground in an agate mortar to homogenize the sample. Data are reported in δ-notation ($\delta^{34}S$) in units of per mil (‰) variations from the Vienna Canyon Diablo Troilite (V-CDT) standard. Analyses were made in a NERC Isotope Community Support Facility, SUERC, Glasgow, Scotland. A comprehensive sulfur isotopic study was conducted on 11 sulfide mineral separates from samples collected from the studied deposits and compared with 6 sulfide mineral separates (Al-Bassam *et al*., 1982). A Thermo delta V isotope ratio mass spectrometer (IRMS) interfaced to a Gas Bench

II, Cornell Isotope Laboratory (COIL), Cornell University, New York, USA has been used for oxygen and carbon isotope analyses. Replicate analyses on the randomly selected samples give a mean deviation of ±0.05‰ for $\delta^{18}O$ and ±0.02‰ for $\delta^{13}C$. All carbonate isotope data are reported in per mill (‰) relative to the Vienna PDB (Pee Dee Belemnite) standard.

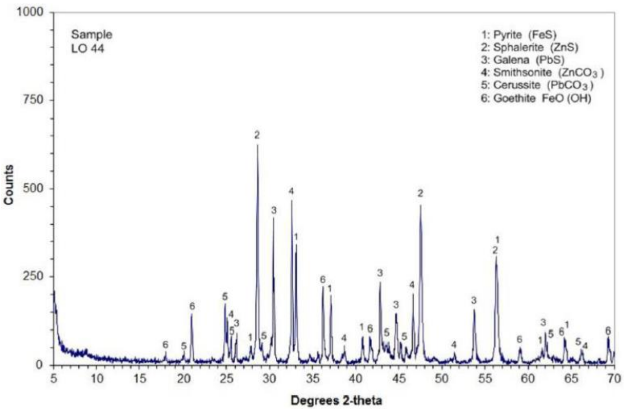

Figure 7) XRD pattern of bulk-ore sample from the Lefan section.

Most fluid inclusions chosen for analyses were considered as primary (contemporaneous with their host minerals) and closely related, spatially and genetically, to the sulfide mineralization. These inclusions are generally small (about 5 µm) and contain no daughter minerals (Fig. 8a, b). Due to the small size of the inclusions, accurate geothermometry is difficult to measured. In addition, some hydrocarbon-rich fluid inclusions are also found in gangue minerals. Fluid inclusions in the late barite generation within the Bekhme Formation at the Lefan Pb-Zn deposit considered as a fingerprint of hydrocarbon generation (Awadh *et al*., 2010).

The salinities of the fluid inclusions in the Dure deposit range from 13.93 wt% NaCl equiv. to >23 wt% NaCl equiv., whereas in the Lefan deposit, they range from 3.06 wt% NaCl equiv. to 14.57 wt% NaCl equivalent (Table 1).

6–Fluid Inclusion

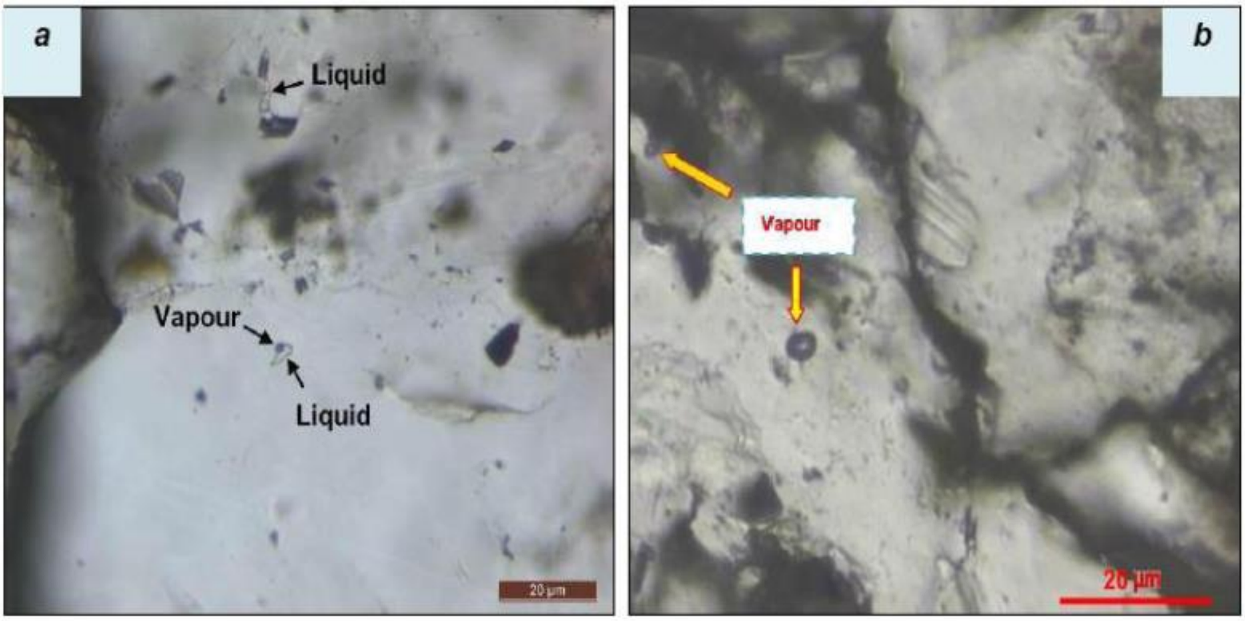

Figure 8) Primary fluid inclusions from the Dure and the Lefan lead-zinc deposits. a) Primary 2-phase fluid inclusions within sphalerite (sample DO 35, the Dure section). b) Primary single phase vapour inclusions within saddle dolomite (sample LO 15, the Lefan section).

The primary fluid inclusions in the Dure and Lefan deposits yielded homogenization temperatures with an average value of 164.22°C, although values range from approximately 60°C to 284°C.

Salinity vs. homogenization temperature diagram of the fluid inclusions in the studied sections has not display limit relationship (Fig. 9).

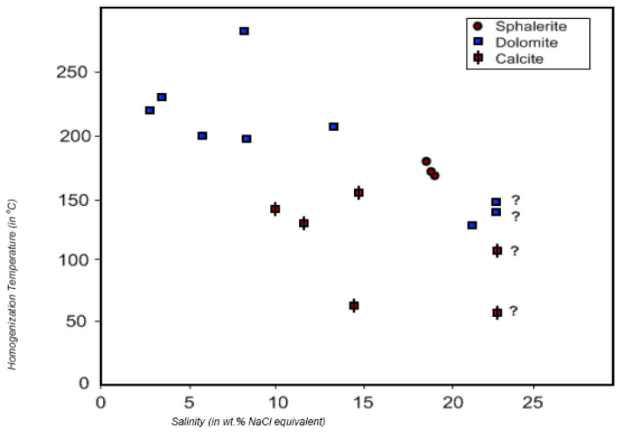

Figure 9) Fluid inclusion salinities vs. homogenization temperatures for the studied deposits (the Dure and the Lefan sections). Question mark means the absolute value of salinity is not determined (i.e., >23).

This scattered relationship between inclusion salinities and homogenization temperatures may be due to a mixing of two solutions; one hot and saline, the other cooler with low salinity (e.g., Taylor *et al.*, 1983). Furthermore, invariant salinities of inclusions are interpreted as evidence of precipitation from a single fluid (Gratz and Misra, 1987). The homogenization temperatures and salinities obtained for inclusions in the studied sections are comparable to those reported for the Mississippi Valley-type (MVT) Pb-Zn deposits (Leach *et al*. 2005, 2010). However, the compositional similarities between the MVT fluid inclusions and oil-field brines are well established and have led to wide¬spread acceptance of a basin-generated origin for the MVT fluids. The high salinity of sedimentary basin brines is explained by the dissolution of evaporites, incorporation of connate bittern brines, or through infiltration of evaporated surface waters (Hanor, 1979).

7–Sulfur Isotopes

The results of the 11 samples of sulfides with 6 from Al-Bassam *et al*. (1982) are provided in Table 2. The δ^{34}S‰ values of sulfides (pyrite, sphalerite and galena) are within the range from -2.6 ‰ to +3.6 ‰ (average=0.8 ‰, n= 13) for Dure, and from +0.47 ‰ to +3.6 ‰ (average=1.8 ‰, n= 4) for Lefan. The average δ34S values of the Dure are slightly lower than that of Lefan (Table 2). The δ^{34}S values of sulfides from Dure and Lefan deposits fall in a narrow range (from -2.6 ‰ to +3.6 ‰, n=17).

Table 1) Homogenization temperatures and salinities of fluid inclusions in sphalerite and carbonate minerals from the Dure (DO-sample) and Lefan (LO-sample) deposits.

Sample No.		T_m °C ice melting temperature	T_h °C homogenization temperature	Salinity Wt% NaCl equivalent	Origin	Mineral
DO 35	1	-14.1	174	17.79	Primary	Sphalerite
	2	-14.3	173	17.96	Primary	Sphalerite
	3	-13.8	183	17.61	Primary	Sphalerite
	4		180		Secondary	Sphalerite
	5		177		Secondary	Sphalerite
	6		179		Secondary	Sphalerite
	7		165		Secondary	Sphalerite
	8		157		Secondary	Sphalerite
DO 28	1	-29.1	144	> 23	Primary	Saddle dolomite
	2	-23.2	147	> 23	Primary	Saddle dolomite
	3	-18.1	128	20.97	Primary	Saddle dolomite
	4		115		Secondary	Saddle dolomite
	5		117		Secondary	Saddle dolomite
	6		97		Secondary	Saddle dolomite
	7		127		Secondary	Saddle dolomite
LO 15	1	-5.3	284	8.14	Primary	Saddle dolomite
	2	-3.2	200	5.11	Primary	Saddle dolomite
	3	-5.3	196	8.14	Primary	Saddle dolomite
	4	-6.9	210	10.36	Primary	Saddle dolomite
	5	-2.2	238	3.55	Primary	Saddle dolomite
	6	-1.8	225	3.06	Primary	Saddle dolomite
	7		193		Secondary	Saddle dolomite
	8		196		Secondary	Saddle dolomite
DO 10	1	-10.1	61	13.93	Primary	Calcite vein
	2	-33.2	59	> 23	Primary	Calcite vein
	3	-35.1	105	> 23	Primary	Calcite vein
	4		45		Secondary	Calcite vein
	5		50		Secondary	Calcite vein
	6		65		Secondary	Calcite vein
	7		74		Secondary	Calcite vein
LO 10	1	-7.8	127	11.46	Primary	Calcite vein
	2	-10.2	145	10.04	Primary	Calcite vein
	3	-10.6	157	14.57	Primary	Calcite vein
	4		71		Secondary	Calcite vein
	5		68		Secondary	Calcite vein

The observed values of sulfur isotope in the Dure (average=0.8 ‰) and Lefan (average=1.8 ‰) cannot necessarily be explained by a magmatic source of sulfur because the field observations and ore microscopy provide no evidences of magmatic activity in their formation. The negative shift of δ34S values can be explained as a result of seawater- or evaporates sulfates, or bacterial reduction. But, this does not exclude the possibility that some of the sulfur might have been derived through the dissolution and leaching of pre-existing sulfide-bearing igneous rocks.

The positive (slightly heavy) $\delta^{34}S$ values suggest that the sulfur was derived from seawater or ancient evaporate and connate water that had undergone subsequent reduction by ferrous iron or organic compounds as indicated by Schütfort (2001) in his study on the San Vicente lead-zinc deposit. Perhaps seawater also became enriched in the light isotope by sulfur being leached from deeper lithologic units during its circulation, as indicated by Eldridge *et al*. (1993), Sherlock *et al*. (1999) and Roth and Taylor (2000). The influence of the enrichment of light sulfur isotopes was more significant for the Dure deposit (average: 0.8 ‰) than for Lefan (average: 1.8 ‰).

Table 2) Sulfur isotope ($\delta^{34}S$) values of the studied lead-zinc deposits. Data of pyrite (n=2), sphalerite (n=2) and galena (n=2) in Dure deposits from AL-Bassam et al. (1982) were also displayed.

Deposit	Sample	Mineral	$\delta^{34}S$ ‰	
Dure	DO 25	Pyrite	0.9	Present study
	DO 22	Pyrite	1.3	Present study
	DO 15	Pyrite	1.6	Present study
		Pyrite	0.2	From Al-Bassam et al. (1982)
		Pyrite	3.6	From Al-Bassam et al. (1982)
	DO 22	Sphalerite	2.4	Present study
	DO 30	Sphalerite	2.0	Present study
		Sphalerite	0.0	From Al-Bassam et al. (1982)
		Sphalerite	-0.4	From Al-Bassam et al. (1982)
	DO 28	Galena	1.8	Present study
	DO 30	Galena	-0.9	Present study
		Galena	-1.8	From Al-Bassam et al. (1982)
		Galena	-2.6	From Al-Bassam et al. (1982)
Lefan	LO 22	Pyrite	3.6	Present study
	LO 15	Sphalerite	1.8	Present study
	LO 15	Galena	1.2	Present study
	LO 18	Galena	0.47	Present study

8–Oxygen and Carbon Isotopes

Bulk samples of dolostone (dolomite) and limestone from unmineralized and mineralized host rocks were analyzed for their carbon and oxygen isotope composition. The carbon isotope results were reported to be relative to the standard PDB. The oxygen isotope results could be reported to be relative to PDB, but usually they are reported to be relative to Standard Mean Ocean Water (SMOW) according to the formula:

δ^{18}OSMOW (at 50 ^{o}C carbonate) = 0.99108 × δ^{18}OSMOW (CO_2) - 8:92 (1

The SMOW values could be converted back to PDB values using the following equation:

δ^{18}OSMOW = 1.03086 × δ^{18}OPDB + 30.86 (from Tucker and Wright, 1990) (2

Carbon and oxygen isotope values for analyzed carbonate host rocks (unmineralized and mineralized samples) are summarized in Table 3.

Barren (Unmineralized) host rock: The δ^{13}CPDB values of carbonate host rocks in the Dure section range from -2.80‰ to 0.60‰ (mean = -0.93‰) and from -0.41‰ to 2.23‰ (mean = 1.15‰) for the Lefan section. The range of δ^{18}OSMOW values for the Dure section samples is between 21.57‰ and 26.24‰ (mean = 22.96‰) and between 22.42‰ and 26.98‰ (mean = 25.47) for Lefan section (Table 3). The small differences in the values of carbon and oxygen isotope in each section can probably be attributed to differences in the depositional environment and subsequent diagenetic processes for each section (Veizer and Hoefs, 1976; Colombie *et al*., 2011).

Mineralized host rock: The δ^{13}CPDB values of mineralized carbonate host rocks in the Dure section range from -2.77‰ to 1.23‰ (mean = -0.41‰) and from -3.34‰ to 1.61‰ (mean = -0.47‰) for the Lefan section. The range of δ^{18}OSMOW values of the mineralized dolomite and limestone for the Dure section is between 18.57‰ and 23.71‰ (mean = 21.41‰) and between 23.51‰ and 25.50‰ (mean = 24.38‰) for the Lefan section (Table 3).

Interpretation: δ^{13}C and δ^{18}O values for the carbonate host rocks in the studied sections vary within a narrow range and fall in the range of marine carbonate reported by He *et al*. (2009) (Fig. 10). The narrow range of the δ13CPDB values probably reflects the resistance of the carbonate host to δ^{13}C depletion during diagenesis. A slight decrease in the δ^{18}OSMOW values for the mineralized dolostone and limestone with respect to unmineralized host rocks in the studied sections (Table 3 and Fig. 10) can be attributed to an isotopic exchange between the carbonate host rock and the mineralizing fluid.

In the stable oxygen isotope studies of ancient carbonate rocks such as the Kurra Chine and Bekhme formations, the possibility of isotopic reequilibration occurred during diagenetic processes, which are capable of altering the original isotopic composition of carbonate should be considered. Nevertheless, the less depleted $\delta^{18}O$ values might represent dolomitization under the influence of a dominantly marine environment, whereas more $\delta^{18}O$ depletion demonstrates the meteoric water realm (Tucker and Wright, 1990). During the stage of mineralization $\delta^{13}C$ values of mineralization stage minerals , i.e. samples DK 58 and DK 65 from the Dure section, samples LB 28 and LB 53 from the Lefan section, tends to be light (Table 3). Light carbon isotopes could have been added to the hydrothermal system from deep-seated magmatic sources or by oxidation of organic matter. A deep-seated magmatic source of carbon is considered to have a uniform $\delta^{13}C \sim -5‰$ (Clark and Fritz, 1997). The range of $\delta^{13}C$ of mineralized samples implies that it could not have been precipitated from such a uniform source (Table 3). In addition such a source for the studied deposits is extremely unlikely because of the lack or absent of igneous activity in the area. Therefore, it is suggested that oxidation of organic matter in marine sediments was active during mineralization. Accordingly, the probable source of carbon has been established as a mixture of the marine sediments plus carbon dioxide formed by the oxidation of organic matter.

9–Source of Metals

During diagenesis a widespread dolomitization, release of metals from metastable carbonate minerals to the pore water is common (Roberts, 1973). Dolomitization of the studied carbonates have occurred so that the released metals could have been retained in the pore water, further increasing the metal content of the basinal brines. Therefore, it is quite possible that some proportion of the metal was derived from carbonate host rocks during their widespread dolomitization. Roberts (1973) and Fuchs (1984) suggested that carbonates themselves were the major source for metal ions and upon mobilization become concentrated forming Zn-Pb deposits. At the Pine Point (Kyle, 1981), the carbonate host rocks are the favored source horizons. Another possible source of Zn and also Pb in the basin could be shale beds within the Kurra Chine Formation and older formations. Dewatering of shale has been favored as a source for metal-bearing fluids (Macqueen, 1976; Coveney and Glascok, 1989; Liaghat *et al*., 2000; Paradis *et al*., 2007). Liaghat *et al*. (2000) suggested that dewatering of shales is a major source for metal-bearing fluids for the Kuh-e-Surmeh Pb-Zn deposit in southwestern Iran. Clay-mineral maturation and dewatering of the siliciclastics (shale) could also have provided Mg for the dolomitization associated with mineralization (e.g., Liaghat *et al*., 2000). Based on these assumptions, it seems reasonable to assume that Zn and Pb were derived from the diagenesis of dolostones and dolomitic limestones or the late stage dewatering of siliciclastic beds or both. Thus, it appears that sediments within the Northern Thrust Zone are capable of producing the necessary amount of metals.

10–Genesis of the Pb-Zn deposit

As assumed by the previous studies (Al-Qaraghuli and Lang, 1978; Al-Bassam *et al*., 1982 and Awadh, 2006) and also by this study, the studied Pb-Zn deposits are of sedimentary origin and have been formed after the lithification of their host rocks (i.e. epigenetic deposits).

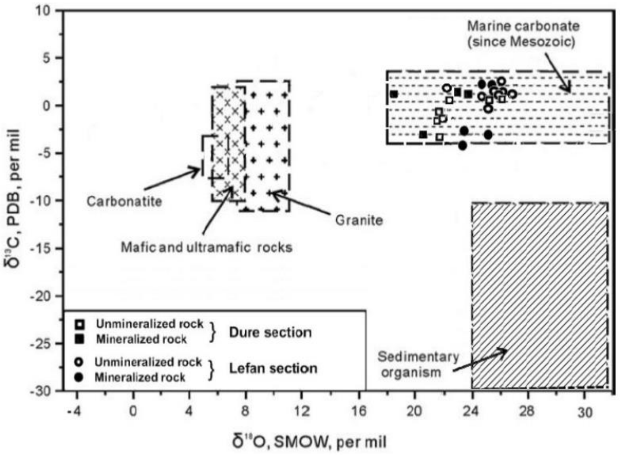

Figure 10) Plot of $\delta^{13}C$ vs. $\delta^{18}O$ of carbonate host rocks of the studied deposits in the Dure, Lefan and Sinjar sections, also showing $\delta^{13}C$ and $\delta^{18}O$ values of the unmineralized and mineralized carbonate rocks in the sections. The fields of carbonatite, mafic and ultramafic rocks, granite, marine carbonate, and marine and non-marine sedimentary organisms are plotted after He et al. (2009).

There are several lines of evidence to suggest basinal brines as the source of ore-forming fluids in the studied sections. Firstly, the fluid inclusions of these deposits have salinities and temperatures mainly within the range of fluids from the MVT deposits (Leach *et al*., 2005, 2010). The second is that the ore deposits display, similar to most basinal brines, low and narrow variations in sulfide $\delta^{34}S$ values (Table 2), probably indicating a single source of sulfur. On account of the lack of magmatic activity, it is realistic to view the rocks in the basin of the studied sections as the source of sulfur.These include evaporite (positive $\delta^{34}S$ values), the strata enriched in organic sulfur (slightly positive to negative $\delta^{34}S$ values), and sedimentary rocks containing diagenetic pyrite. Third, carbon and oxygen isotope values in the carbonate-host rocks are generally characterized by relatively lower $\delta^{18}O$ and higher $\delta^{13}C$, which require involvement of marine carbonates and organic matter in the basin to supply carbon and oxygen (Fig. 10). In addition, the fact that hydrocarbon-rich fluid inclusions are found in some gangue minerals, and a late generation of barite (Awadh *et al*., 2010) also testifies the probability that basinal brines were the source of ore-forming fluids. Comparing with typical basinal brines, some fluid inclusions in the studied deposits yielded relatively lower salinities (<10 wt.% NaCl equiv.). However, the low-salinity of these fluid inclusions shows a positive correlation with their Th values, suggesting a possible mixing between meteoric water and basinal brines.

Table 3) Carbon ($\delta^{13}C$) and oxygen ($\delta^{18}O$) isotope values of carbonate host rocks in the studied sections. DK samples from Dure section and LB samples from Lefan section. LSh 1 is one sample from Shiranish Formation from Dure section.

Sample	Lithology	$\delta^{13}C_{PDB}$ ‰	$\delta^{18}O_{PDB}$ ‰	$\delta^{18}O_{SMOW}$ ‰
DK 90	Dolomitized lime-mudstone	-1.05	-4.48	26.24
DK 84	Black dolomitic shale	0.60	-8.48	22.12
DK 80*	Fine dolomitized limestone	1.23	-7.71	22.91
DK 70*	Brecciated dolostone	1.16	-6.94	23.71
DK 65*	Saddle dolomite	-1.25	-11.93	18.56
DK 58*	Smithsonite ($ZnCO_3$)	-2.77	-10.09	20.46
DK 45	Coarse dolomitized limestone	0.59	-5.49	25.20
DK 32	Coarse gray dolostone	-1.57	-9.01	21.57
DK 25	Bioclastic lime-mudstone	-1.30	-8.70	21.89
DK 18	Brecciated dolomitic limestone	-2.80	-8.48	22.12
DK 10	Bioclastic lime-wackstone	-1.00	-9.01	21.57
LSh 1	Packstone (limestone)	0.31	-4.53	26.19
LB 68	Coarse dolostone	1.93	-8.19	22.42
LB 64	Dolomitized lime-wackstone	-0.41	-5.67	25.01
LB 60	Dolomitized lime-wackstone	2.23	-4.83	25.88
LB 55	Dolomitized lime-wackstone/packstone	1.37	-5.37	25.32
LB 53*	Dolostone with saddle dolomite	-2.53	-7.04	23.61
LB 35*	Dolomitized lime-packstone	1.61	-5.20	25.50
LB 32*	Dolomitized lime-grainstone	0.96	-6.15	24.52
LB 31*	Recrystallized limestone	0.94	-5.93	24.75
LB 28	Dolomitized lime-grainstone	-3.34	-7.13	23.51
LB 25	Dolomitic limestone	1.28	-3.77	26.98
LB 20	Recrystallized lime-wackstone	1.13	-5.91	24.77
LB 17	Dedolomitized dolostone	1.24	-4.87	25.84
LB 12	Rudist boundstone (limestone)	1.27	-3.94	26.80

*: Mineralized samples
Others are unmineralized samples

This study suggests that the Pb-Zn deposits are concentrated from basinal brines (marine waters), which travelled along deep cracks and faults at the beginning of the orogeny event. At depth, the fluid heated up and dissolved metals from rocks during its ascent, and when the concentration of metal ions increased sufficiently then deposition occurred. This process and structural features such as faults and cracks, together with wall-rock permeability and reactivity would be the eventual controlling factors of mineralization, geometry of the ore bodies and the alteration. According to Leach and Sangster (1993), fluids migrating through deep portions of the sedimentary basin become heated and dissolve rock components, and are then forced upward toward basin margins due to orogenic compaction, crustal thickening and faulting. At the scale of the studied deposit, mineralization tends to occur in fractures and solution-collapse features formed during the uplift of platform-carbonate sequences accompanying plate convergence. Thus, the preferred genetic model for the concentration of the ore metals at the studied carbonate rocks involved basin dewatering due to compaction and regional tectonism and expulsion of the basin-derived fluids into the brecciated, karstificated and highly porous recrystallized and dolomitized rocks of the Kurra Chine and, Bekhme formations.

11–Conclusions

The studied Pb-Zn deposits are of simple mineralogy and occurred mainly in deformational structures as stratabound, open-space fillings, veins, and dissemination ore bodies and show no association with igneous activities.

Based on field relationships, petrography and mineralogy, fluid inclusions, and stable isotopic data, the Pb-Zn ore bodies in both the Dure and Lefan were deposited by the same processes that led to the formation of massive, fracture-controlled ores, which are interpreted as part of a feeder vein system for the deposits.

The ores are epigenetic and were formed by deeply circulating high temperature mineralizing fluids (brines) within the source basin or by tectonic processes, which possibly leached metals from either the diagenesis of host rocks or the dewatering of deeper buried siliciclastic beds or both. The studied Pb-Zn deposits seem to display characteristics consistent with the Mississippi Valley Type (MVT) deposits, but differ with respect to the iron sulfides occurring in greater amounts at the Dure section.

Acknowledgments:

The authors thank members of Iran Mineral Processing Research Center (IMPRC), NERC Isotope Community Support Facility, SUERC, Glasgow, Scotland and Cornell Isotope Laboratory (COIL), Cornell University, New York, USA for facilitating fluid inclusion, sulfur isotope and Carbon/oxygen isotopes analyses, respectively, for the research. Thanks also to the Ms. Israa Shingaly for excellent computer assistance.The author would like to thank Dr. J. Bejaoui, Dr. N. Jemmali and an anonymous reviewer for their appreciate comments which help him to improve manuscript.

References:

Akef, A., 1972. Geological environments and factors affected the formation of Duri-Serguza lead and zinc ore-bodies.Second Iraqi geological conference, Baghdad, Iraq.

Al-Ameri, T.K., Al-Dolaimy, Q.H., Al-Khafaji, A.J. 2009. Palynofacies and hydrocarbon generation potential of the upper Triassic Kurrachine Formation and lower part of the Baluti Formation, Mosul Block, Northwestern Iraq. Arabian Journal of Geosciences: 2, 273–283.

Al-Bassam, K., Hak, J., Watkinson, D., 1982. Contribution to the origin of the Serguza lead-zinc-pyrite deposit, Northern Iraq. Mineralium Deposita: 17, 133–149.

Al-Qaraghuli, N., Lang, H., 1978. Geochemical and mineralogical investigation of pyrite-sphalerite-galena deposit in Duri-Serguza area, northern Iraq. Journal of Geological Society of Ira: 11, 46–66.

Alsharhan, A.S., Nairn, A.E. 1997. Sedimentary basins and petroleum geology of the Middle East. Elsevier publisher, Amsterdam, 843 P.

Aqrawi, A.A.M., Goff, J.C., Horbury, A.D., Sadooni, F.N. 2010. The Petroleum Geology of Iraq. Scientific Press Ltd, 424 P.

Awadh, S.M. 2006. Mineralogy, geochemistry and origin of the zinc–lead–barite deposits from selected areas from north of Zakho, Northern Iraq. Ph.D. Thesis, University of Baghdad, 192 P.

Awadh, S.M, Al-Ameri, T.K., Jassim, S.Y., Bayraktutan, M.S. 2010. Fluid inclusions usage for assessing oil migration in Duhok, north Iraq. Positioning, 1, 42–49.

Buday, T., 1980. The regional geology of Iraq, Stratigraphy and Paleogeography,Volume I. Dar Al-Kutub publishing. Mosul University, Iraq, 445 P.

Buday, R.T., Jassim, S.Z., 1987. The regional geology of Iraq, Tectonism, Magmatim and metamorphism, Volume 2. Geological Surveying and Mineral Investigation, Baghdad, 352P.

Clark, I., Fritz, P., 1997. Environmental Isotopes in Hydrogeology, Lewis Publishers, New York, 328 P.

Colombiè, C., Lècuyer, C., Strasser, A. 2011. Carbon- and oxygen-isotope records of palaeoenvironmental and carbonate production changes in shallow-marine carbonates (Kimmeridgian, Swiss Jura). Geological Magazine: 148, 133–153.

Coveney, R.M., Glascock, M.D. 1989. A review of the origins of the metal-rich Pennsylvanian black shales, central USA, with an inferred role for basinal brines. Applied Geochemistry: 4, 317–367.

Dickson, J.A. 1965. Carbonate identification and genesis as revealed by staining. Journal of Sedimentary Petrology: 36, 13–21.

Dunnigton, H.V., Wetzel, R., Morton, D.M. 1959. Lexique stratigraphique international, vol. III, Asie, Iraq. International Geology Congress Commission de Stratigraphique, 3, Fasco.10a. 333 P.

Eldridge, C.S., Williams, N., Walshe, J.L. 1993. Sulfur isotope variability in sediment-hosted massive sulfide deposits as determined using the ion microprobe SHRIMP: II. A study of the H.Y.C. deposit at McArthur River, Northern Territory, Australia. Economic Geology: 88, 1–26.

Flügel, E. 2004. Microfacies of Carbonate Rocks: Analysis, Interpretation and Application. Verlag Berlin Heidelberg, Springer, 976 P.

Fuchs, Y. 1984. Migration of fluids during diagenesis: An ore-forming process in carbonate rocks, In: Wauschkuhn, A., Kluth, C., Zimmermann, R. (Eds.), Syngenesis and epigenesis in the formation of mineral deposits. Springer, Berlin-Heidelberg-New York, pp. 287–293.

Gratz, J.F., Misra, K.C. 1987. Fluid inclusion study of the Gordonsville zinc deposit, central Tennessee. Economic Geology: 82, 1790–1804.

Hanor, J.S. 1979. The sedimentary genesis of hydrothermal fluids, In: Barnes, H. L. (Ed.), Geochemistry of hydrothennal ore deposits. New York, Wiley Inter-science publishers, pp. 137–142.

He, L., Song, Y., Chen,K., Hou, Z., Yu, F., Yang, Z., Wei, J., Li, Z., Liu, Y. 2009. Thrust-controlled, sediment-hosted, Himalayan Zn–Pb–Cu–Ag deposits in the Lanping foreland fold belt, eastern margin of Tibetan Plateau. Ore Geology Reviews: 36, 106–132.

Jassim, S. Z., Goff, J.C. 2006. Geology of Iraq, Published by Dolin, Prague and Moravian Museum, Brno. Printed in the Czech Republic, 341 P.

Kyle, J.R. 1981. Geology of the Pine Point lead-zinc district. In: Wolf, K. H. (ed.): Handbook of strata-bound and stratiform ore deposits. New York, Elsevier, 9, pp. 643–741.

Leach, D.L., Sangster, D.F. 1993. Mississippi valley-type lead–zinc deposits, In: Kirkham R. V., Sinclair W. D., Thorpe R. I., Duke J. M. (Eds), Mineral deposit modeling. Geological Association of Canada, Special Paper: 40, 289–314.

Leach, D.L., Sangster, D.F., Kelly, K.D., Large, R.R., Garven, G., Allen, C.R., Gutzmer, J., Walters, S. 2005. Sediment-hosted lead–zinc deposits: A global perspective. Economic Geology: 100th Anniversary Volume, 561–607.

Leach, D. L., Taylor, R.D., Fey, D.L., Diehl, S. F., Saltus, R.W. 2010. A Deposit Model for Mississippi Valley-Type Lead-Zinc Ores, Chapter A of Mineral Deposit Models for Resource Assessment, USGS, Sci. Inv. Report 5070-A, p. 52.

Liaghat, S., Moore, F., Jami, M. 2000. The Kuh-e-Surmeh mineralization, a carbonate-hosted Zn-Pb deposit in the Simply Folded Belt of the Zagros Mountains, SW Iran. Mineralium Deposita: 35, 72–78.

Macqueen, R.W. 1976. Sediments, zinc and lead, Rocky Mountain Belt, Canadian cordillera. Geoscience Canada: 3, 71–81.

Paradis, S., Hannigan, P., Dewing, K. 2007. Mississippi Valley-Type lead-zinc deposits,In: Goodfellow, W.D.(Ed.), Mineral deposits of Canada: A synthesis of major deposit-types, district metallogeny, the evolution of geological provinces, and exploration methods. Geological Association of Canada, Mineral Deposits Division, Special Publication: 5, 185–203.

Roberts, W.M. 1973. Dolomitization and the genesis of the Woodcutters lead-zinc prospect, Northern Territory, Australia.Mineralium Deposita: 8, 35–56.

Roth, T., Taylor, B.E. 2000. Sulfur isotope and textural zoning of pyrite in mudstone about the polymetallic Eskay Creek Deposit, Northwestern British Columbia, Canada. Volcanic Environments and Massive Sulfide Deposits International Conference, Hobart, Tasmania, pp. 16–19.

Schütfort, E.G. 2001. The Genesis of the San Vicente Lead Zinc Rhythm ite Deposit, Peru -a Petrologic, Geochemical, and Sulfur Isotope Study. M.Sc. Thesis, Oregon State University, 136 P.

Sharland, P.R., Archer, R., Casey, D., Davies,R.B., Hall, S.H., Heward, A.P., Horbury, A.D., Simmons, M.D.2001. Arabian Plate Sequence Stratigrpahy. GeoArabia, Special Publication 2, Gulf Petrolik. Manama, Bahrain, 371P.

Sherlock, R.L., Roth, T., Spooner, E.T., Bray, C.J. 1999. Origin of the Eskay Creek precious metal-rich volcanogenic massive sulfide deposit: Fluid inclusion and stable isotope evidence. Economic Geology: 94, 803–824.

Sissakian, V. K., 2000. Geological map of Iraq. GEOSURV, Baghdad, Iraq.

Taylor, M., Kesler, S.E., Cloke, P.L., Kelly, W.C. 1983. Fluid inclusion evidence for fluid mixing, Mascot-Jefferson City zinc district, Tennessee. Economic Geology: 78, 1425–1439.

Tucker, M.E., Wright, V.P. 1990. Carbonate Sedimentology. Blackwell Scientific Publishing, Oxford, 482 P.

Vanecek, M.1972.The principal metallogenic features of Iraq. Acta Universitatis Carolinae-Geologica, Prague: 3, 237–252.

Veizer, J., Hoefs, J. 1976. The nature of O^{18}/O^{16} and C^{13}/C^{12} secular trends in sedimentary carbonate rocks. Geochimica et Cosmochimica Acta: 40, 1387–1395.

Wilson, J.L. 1975. Carbonate Facies in Geological History. Springer-Verlag, New York Heidelberg Berlin, 471 P.